A Comprehensive, Zero-Setting Algorithm to Detect Secondary Arc Extinction

Emma Clawson, David Schmidt, Sajal Kumar Harmukh, Jordan A. Bell, Omar A. Oliveros, Jean León Eternod, Jacob Smith, and Colton Hubbell
Schweitzer Engineering Laboratories, Inc.

Presented at the
79th Annual Georgia Tech Protective Relaying Conference
Atlanta, Georgia
April 15–17, 2026

Originally presented at the
79th Annual Conference for Protective Relay Engineers, March 2026

A Comprehensive, Zero-Setting Algorithm to Detect Secondary Arc Extinction

Emma Clawson, David Schmidt, Sajal Kumar Harmukh, Jordan A. Bell, Omar A. Oliveros, Jean León Eternod, Jacob Smith, and Colton Hubbell, *Schweitzer Engineering Laboratories, Inc.*

***Abstract*—Single-pole tripping and reclosing is used to maintain power transfer and improve transient stability when clearing single-line-to-ground faults. While the single phase is open, the healthy phases can sustain the ionized channel created by the primary fault, resulting in a secondary arc. The arc must extinguish before reclosing to successfully re-energize the open phase.**

Typically, the autoreclosing open interval time is set to a fixed, conservative dead time to allow sufficient time for the secondary arc to extinguish. This is simple, but not optimal. Secondary arc extinction depends on several deterministic and random factors and may occur well before the end of the dead time. Conversely, for a permanent fault, the arc will not extinguish by the end of the dead time. Detection of secondary arc extinction can further improve system stability by reclosing faster, and detecting a persistent fault on the open phase can help prevent stressing the system again by blocking reclosing and tripping three pole to extinguish the fault.

The authors previously proposed an algorithm to detect secondary arc extinction and permanent faults. For lines with no shunt reactors, this algorithm relied on mutual coupling line parameters. However, these parameters may not be easy to determine for different types of parallel line configurations. Further, the lines may have series capacitors and/or grounded three-legged or four-legged shunt reactors, which pose their own unique problems.

This paper presents a single, comprehensive algorithm that accommodates all previously stated configurations without requiring any user settings. The algorithm presented in this paper goes back to first principles to identify unique signatures in the open-phase voltage. These signatures can be used to detect secondary arc extinction for any line configuration. The performance of the algorithm is validated against field events and simulations.

I. Introduction

Single-pole tripping and reclosing (SPTR) is used to maintain power transfer via two healthy phases while clearing a single-line-to-ground fault. However, inductive and capacitive coupling between the faulted phase and the two healthy phases can prolong the primary fault arc after the single pole opens (secondary arc). For a successful reclose, the secondary arc must be extinguished before the line is re-energized. If a sustained secondary arc can be detected at the end of the open interval, then the reclose onto the fault can be prevented, limiting the stress to the system, and the single-pole open can be converted to a three-pole trip.

In a previous paper, the authors proposed an algorithm that detected the extinction of the secondary arc for lines where the mutual coupling parameters were known and for lines that were compensated with a four-legged shunt reactor bank (three-phase reactors and a neutral reactor) [1]. This paper takes that previous algorithm a step further, tackling the challenge of detecting a secondary arc extinction (SAE) on mutually coupled lines where the mutual coupling parameters are difficult to determine, lines with series compensation, and lines with grounded three-legged shunt reactors that do not have a neutral reactor.

Accurate knowledge of the line parameters for mutually coupled lines may be possible for two lines that share the same right-of-way and are mutually coupled for their entire length. While these lines may be common in the power system, they are certainly not the only types of mutually coupled lines. Some lines are mutually coupled for only a portion of the line and connect to different substations at the other end. Others are mutually coupled only for a middle portion of the line and do not share a substation at either end. Many lines share a right-of-way with one or many lines.

All these potential configurations make calculating accurate line parameters and the mutual coupling parameters from other lines nearly impossible. Instead of attempting the simulation and analysis of many of these potential scenarios, the authors decided to simplify the problem by going back to first principles.

Lines that are shunt-reactor compensated with only three reactors behave similarly to lines compensated with four reactors. However, the ringing frequency for three-reactor-compensated lines approaches the fundamental frequency at lower compensation values than for four-reactor-compensated lines and cannot be distinguished as ringing, which the algorithm in [1] used to determine that the secondary arc had extinguished. In those scenarios, another complementary method must be added.

Section II of this paper discusses the theoretical principles behind detecting the unique signatures used to determine that the secondary arc has extinguished. Section III describes how these signatures are practically used in an algorithm. Section IV presents the response of the algorithm to arcs simulated on different line configurations using real-time digital simulation and how the algorithm responds to field events.

II. Theoretical Analysis

A. DC Offset After Secondary Arc Extinction

It was observed during SPTR simulations in transmission lines that a large, slowly decaying dc component was present on the primary system when the secondary arc extinguished. However, this dc component will not pass through the coupling capacitor voltage transformer (CCVT). The next section explores the CCVT response to this dc in more detail. This section describes why a dc offset occurs when a secondary arc is extinguished.

Consider the simplified circuit shown in Fig. 1 for an uncompensated line with a secondary arc after the single-pole trip [2]. Line impedance has been ignored for this analysis. The average voltage of the two healthy phases is represented by V_{Avg}. The voltage of the open phase is represented by V_{Opn}. The variable C_G refers to the phase-to-ground capacitance, C_M refers to the mutual phase capacitance, and R_{ARC} refers to the fault arc resistance, which is shown as a variable resistance that increases with time as the arc lengthens. The reactance values due to C_M and C_G are much larger than that of the fault resistance; therefore, the circuit is mostly capacitive and R_{ARC} acts almost as a short across C_G. Typically, the reactance of C_M and C_G is on the order of hundreds of kilohms, and the fault resistance is on the order of one to hundreds of ohms [3].

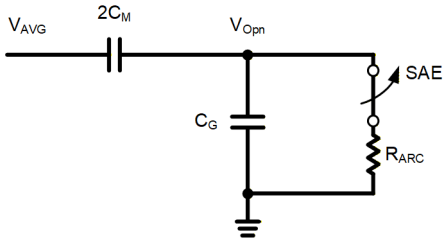

Fig. 1. Simplified open circuit with a secondary arc.

The arc will always extinguish at a secondary arc current zero crossing. When the secondary arc current crosses zero, the voltage across the arc, and therefore across C_G, is zero. Because the circuit is mostly capacitive when the arc current is zero, the voltage across $2C_M$ is at its peak; therefore, V_{Avg} is also at its peak. This is the t^- condition of the circuit.

At t^+, the arc extinguishes and so R_{ARC} is removed from the circuit. This leaves a capacitive voltage divider across $2C_M$ and C_G. With this new circuit configuration, the voltage across C_G is proportional to the V_{Avg}. Because the voltage across C_G at t^- is zero and the voltage across C_G at t^+ should be proportional to the peak of V_{Avg} when the switch is open, a decaying dc transient is introduced to the circuit to fulfill the boundary conditions (a capacitor cannot have a sudden voltage change across it). The initial magnitude of the dc component is approximately equal to V_{DC} as shown in (1).

$$V_{DC} = \left(\frac{2C_M}{2C_M + C_G} \right) V_{Avg} \tag{1}$$

This dc voltage decays very slowly with the high time constant dictated by the distributed shunt conductance and shunt capacitance. Note that this dc voltage will always appear after an arc extinction because of the sudden voltage change imposed across the capacitor C_G. If properly used, this can provide a powerful way to detect the extinction of a secondary arc.

B. Coupling Capacitor Voltage Transformer Behavior With DC Signals

The slow-decaying dc, which occurs after SAE, presents itself as almost a step dc signal to the CCVTs, which do not allow dc to pass through because of the transformer inside of them. This presents a challenge in using the slow-decaying dc for detecting SAE.

However, the CCVTs cannot remove the dc instantaneously. Different types of CCVTs respond differently to a step dc signal depending on their internal parameters; however, they all take time to eliminate the dc. This can be better understood by analyzing the eigenvalues from the transfer function of the CCVTs. In [4], two types of CCVTs have been considered: "extra-high-C CVT" and "high-C CVT." The difference between them is the size of the coupling capacitor. The response to an "almost" step signal will be dictated by the respective CCVT eigenvalues.

The "extra-high-C CVT" eigenvalues are all real and negative, which indicates a unipolar decaying dc-type response with multiple time constants. The eigenvalues of the "high-C CVT" are all complex pairs with negative real parts, indicating a decaying oscillatory response. The higher frequency eigenvalues have a frequency greater than 60 Hz, but decay quickly. The lower frequency eigenvalues have a frequency less than 60 Hz and decay more slowly. The superimposition of these two components defines the CCVT response. It is important to note that the higher frequency component decays quickly before it can cause additional zero crossings.

Fig. 2 shows the simulated response of two CCVT models to a dc step input of 100 V (100 V is a representative step input chosen to facilitate interpretation of the response as a percentage of the input, see Section VI.A for additional details) [5]. CCVT1 represents an "extra-high-C CVT" with a decaying exponential-type response, while CCVT2 represents a "high-C CVT" (see Section VI.A for additional details). As shown by the CCVT2 response, the high-frequency component decays rapidly and the low-frequency response is less than 60 Hz (approximately 10 Hz).

Based on the previous observations, a simple algorithm can be designed that measures the duration of the extracted open-phase voltage dc (of either polarity; resultant positive polarity example in Fig. 2). For an "extra-high-C CVT," with all real and negative eigenvalues, the extracted dc will not cross zero for a long time, which is dictated by the slowest time constant. For a "high-C CVT," this duration will be dictated by the slower decaying lower frequency eigenvalue (less than 60 Hz). Thus, if the duration between the zero crossings of the filtered voltage signal (filtered to remove fundamental and higher frequencies) is more than half of the fundamental period, then it can indicate that an "almost" step dc was encountered at the inputs of CCVT. For Fig. 2, the CCVT1 response crosses zero 19 ms after the dc step input is applied and the CCVT2 response crosses zero 24 ms after the dc step is applied. This gives

adequate time for an algorithm to determine that the previously described dc step input has occurred on the primary system.

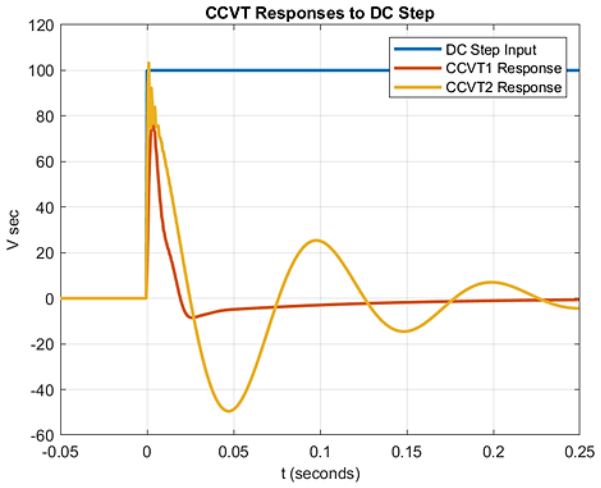

Fig. 2. CCVT response to dc step change.

C. *Ringing Analysis for Parallel Compensated Lines*

A detailed analysis of ringing is covered in Section X of [1]. These principles do not change when the line is a parallel line. The open-phase voltage may be different due to different mutual impedances between the healthy phases of the same line and the parallel line, but on the open phase, the circuit in Fig. 3 is the same as in [1].

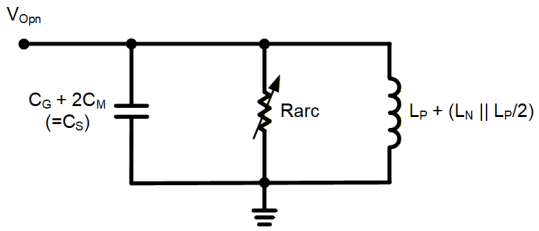

Fig. 3. Equivalent circuit for ringing with four-legged reactor bank.

In this circuit, L_P refers to the phase reactor inductance, L_N refers to the neutral reactor inductance, and C_S is the self capacitance of the open phase. For simplicity, this analysis assumes that the lines are transposed. With the introduction of a parallel line, the self capacitance will change, but the circuit topology will not.

When the arc is present, V_{Opn} is the voltage across the arc resistance. Because the arc is resistive, when the arc extinguishes at a current zero crossing, V_{Opn} is also zero. When V_{OPN} is zero, there is no energy stored in the capacitor, but maximum energy is stored in the inductor. Therefore, when the arc resistance is removed, the inductor energy discharges into the capacitor, resulting in resonance.

D. *Three-Reactor-Compensated Line Analysis*

In [1], the authors proposed a method to detect SAEs on shunt-reactor-compensated lines by detecting a subsynchronous component in the open-phase voltage that occurs due to ringing between the line shunt capacitance and the shunt reactors after arc extinction, as described in the previous subsection (see Section II.C). Stable measurement (i.e., less than 0.5 Hz deviation over five consecutive measurements) of a subsynchronous frequency was used to declare SAE detection (SAED). Furthermore, the measured ringing frequency was used to estimate the magnitude of the ringing component in the open-phase voltage. The estimated magnitude of the subsynchronous component was then used to dynamically adjust the threshold of the harmonic detection function to compensate for filter leakage and to avoid incorrectly identifying ringing frequencies as higher-order harmonics associated with the presence of a secondary arc. The method was developed for transmission lines compensated with four-legged shunt reactors. This section extends that methodology to transmission lines compensated with three-legged shunt reactors (shunt compensation without a neutral reactor and with a grounded neutral point).

Section X of [1] provides a derivation of the equivalent circuit and equations to analyze ringing in a four-legged shunt-reactor-compensated line. For a three-legged shunt-reactor-compensated line, the analysis is similar, but it is simpler with only the phase reactance parallel to C_S. Fig. 4 shows the reduced equivalent circuit.

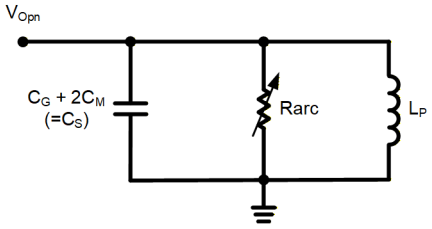

Fig. 4. Equivalent circuit for ringing with three-legged reactor bank.

Based on this equivalent circuit, the ringing frequency as a function of the per-unit compensation factor and the line capacitances is shown in (2) (see Section VI.B for details).

$$F_{RING\_PU} = \frac{F_{RING}}{F_{NOM}} = \sqrt{Comp_{PU}\left(1 + \frac{C_M}{C_S}\right)} \qquad (2)$$

In (2), C_M and C_S refer to the mutual and self shunt capacitances of the transmission line, respectively, and $Comp_{PU}$ refers to the level of shunt reactor compensation, expressed in per unit of the positive-sequence shunt capacitance (C_1) of the transmission line.

For a given line configuration (indicated by the C_M/C_S ratio), as the per-unit compensation factor ($Comp_{PU}$) increases, the ringing frequency increases. If the ringing frequency approaches the nominal frequency (as it will for more heavily compensated lines), it becomes difficult to distinguish the ringing frequency from the fundamental, which challenges the algorithm. However, inspection of the electrostatic component of the open-phase voltage in these scenarios offers an alternative.

Fig. 5a shows the simplified circuit for estimating the electrostatic component of the open-phase voltage for a three-legged shunt-reactor-compensated line following an arc extinction and Fig. 5b shows the reduced equivalent circuit.

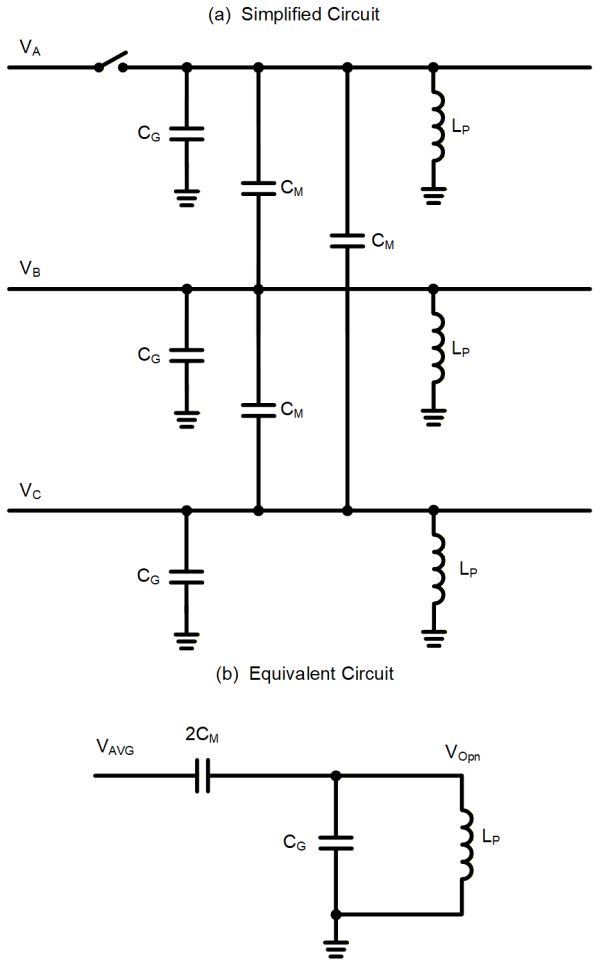

Fig. 5. Transmission line with three-legged shunt reactor bank.

Based on this equivalent circuit, the open-phase voltage magnitude as a function of the per-unit compensation factor and the line capacitances is as shown in (3). For additional information, refer to Section VI.B.

$$\left|V_{Opn\_PU}\right| = \frac{\left|V_{Opn}\right|}{V_{NomLN}} = \left|\frac{\frac{C_M}{C_S}}{1 - Comp_{PU}\left(1 + \frac{C_M}{C_S}\right)}\right| \quad (3)$$

The negative sign on the per-unit compensation factor in the denominator shows that for a given line configuration (indicated by the C_M/C_S ratio), as the compensation factor increases, the open-phase voltage magnitude increases. Furthermore, there is a critical compensation level at which the denominator becomes zero and the voltage magnitude asymptotes. For compensation levels greater than the critical level, the open-phase voltage magnitude decreases as the compensation level increases.

Equation (2) can be rearranged to express $Comp_{PU}$ as a function of C_M/C_S when F_{RING_PU} is 1 (the boundary condition for which ringing detection is not possible). The relationship is given in (4).

$$Comp_{PU} = \frac{1}{1 + \frac{C_M}{C_S}} \quad (4)$$

This is the condition that makes the denominator in (3) evaluate to zero.

The increase in the electrostatic open-phase voltage, when the ringing frequency is near the fundamental, allows a high-set voltage magnitude detector to substitute for the ringing detection in those cases where ringing cannot be detected (i.e., where it is too close to the fundamental). The high magnitude also raises the harmonic detection threshold, which is based on a percentage of the phasor magnitude, so that harmonics introduced by ringing do not block SAED.

Fig. 6 shows the estimated per-unit ringing frequency from (2) and the per-unit electrostatic open-phase voltage magnitude from (3) for a transmission line with $C_M/C_S = 0.2$ and varying levels of shunt compensation. When the compensation increases to a point where the ringing frequency is too close to the fundamental frequency to be effectively isolated, the electrostatic component of the open-phase voltage becomes very large.

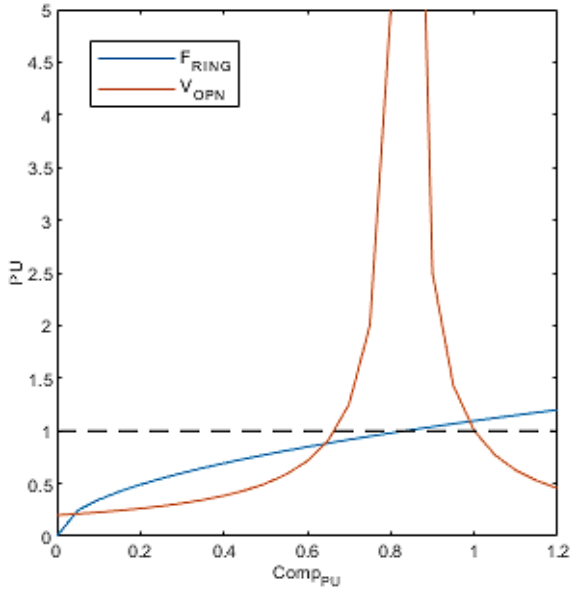

Fig. 6. Estimated ringing frequency (pu) and voltage magnitude (pu) for $C_M/C_S = 0.2$.

E. Series-Compensated Lines

The following three cases are the possible actions to take for series-capacitor-compensated lines when a single-phase trip action is performed:

1. Single-phase trip and reclose proceeds without any control action on the series capacitors.
2. Only the series capacitor of the faulted phase is bypassed from the single-phase trip and then inserted after the reclose.
3. All three phases of the series capacitors are bypassed from the single-phase trip and then inserted after the reclose.

Several papers (e.g., [6] and [7]) have shown that the presence of series capacitors (SCs) when opening a breaker can lead to an increase in transient recovery voltage (TRV) and the rate-of-rise of recovery voltage (RRRV) inside the breaker. This can cause damage to the breakers if they are not properly sized to account for the increased values of TRV and RRRV. That is why utilities typically implement a fast bypass of the series capacitors from line protection operations before the breakers are opened and delayed insertion after the breakers are closed. Therefore, Cases 2 and 3 are more common.

In Case 3, where series capacitors of all three phases are bypassed, there will be no impact from the series capacitors to SAE. In Case 2, the presence of the series capacitors in the unfaulted phases increases the flow of current in those phases for the same load angle difference between two ends, which is due to a net reduction of the effective line impedance. Consequently, this leads to an increased electromagnetic coupling voltage being induced in the open phase. The electromagnetic voltage may either be in phase or opposite phase to the capacitively induced electrostatic voltage [1] and may increase or decrease the open-phase voltage. From the simulations shown in [1] (refer to Section II.C), the maximum decrease was found to be approximately 25 percent, which is not prohibitive for the dc detection algorithm (see Section III.A), which uses a very small threshold (higher than noise level) for a dc value to be counted as positive or negative. However, for Cases 2 and 3 it is possible that the line breaker might open before the series capacitors could bypass because of either a communications delay in the bypass signal, slow operation of the bypass breaker, or other factors. In such situations, the bypass may get delayed by a short time duration after breaker opening.

For Case 1 (where no control action is taken for the series capacitor) and for Cases 2 and 3 (where there is a low-probability event of the series capacitor not bypassing in time), the impact must be considered regarding the presence of the faulted phase series capacitor on the open-phase voltage. Therefore, the impact was analyzed for uncompensated (not shunt reactor compensated) and shunt-reactor-compensated transmission lines using MATLAB and Simulink to perform simulations, which is discussed as follows.

For an uncompensated line (not shunt reactor compensated), the series capacitance percent compensation was changed from 0 to 80 percent in 10 percent increments, while also changing the line loading, fault location, and series capacitor location. Three options for the series capacitor location were considered: local, remote, and capacitors split equally between local and remote. The impact on peak dc was observed in all cases against changing series capacitor compensation (SCC) levels. The behavior was not consistent, as shown in Fig. 7. The peak dc value increased with increasing SCC for some cases, as in Fig. 7a; was erratic for other cases, as in Fig. 7b; and decreased for various other cases, as in Fig. 7c. It is important to note that a higher initial value of the dc offset works in favor of the algorithm and increases the detection margin. The maximum decrease in peak dc was observed to be approximately 14 percent (it decreased from 36 kV to 30.7 kV for a 400 kV system), which is not significant enough to cause the algorithm to miss detecting SAE.

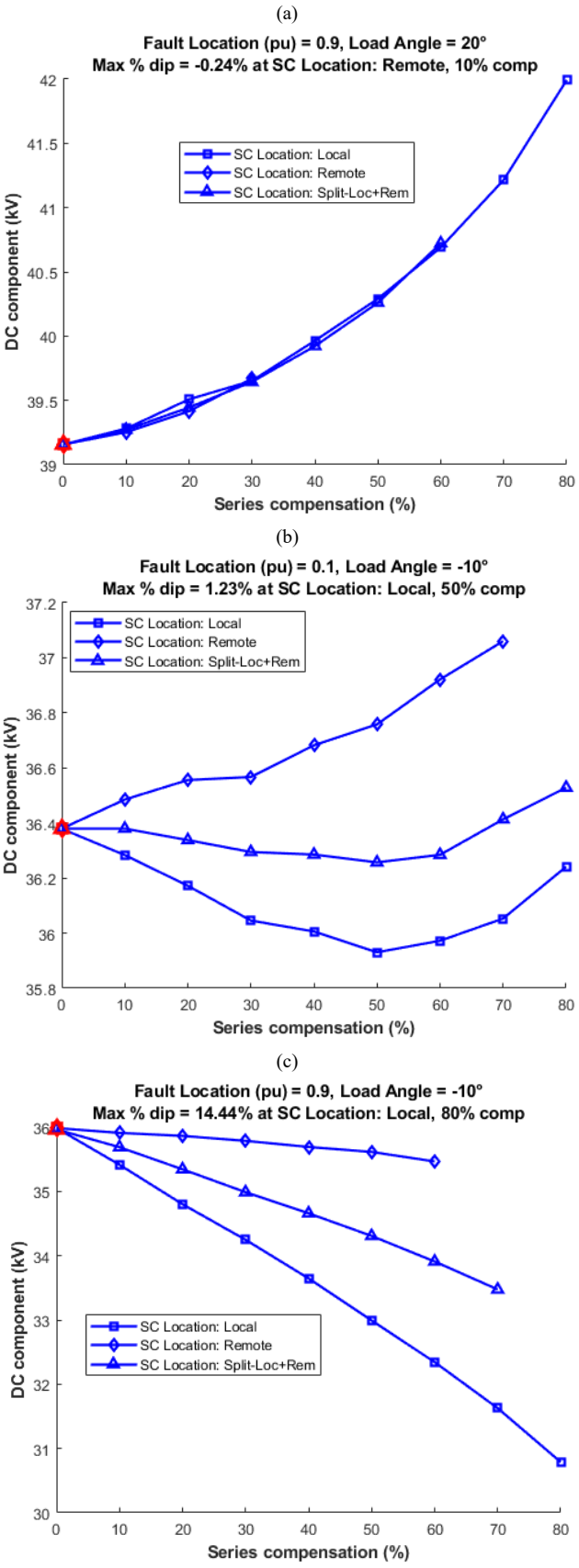

Fig. 7. Peak dc for various conditions.

For the shunt-reactor-compensated lines, where ringing detection is used to detect SAE, verification was made through mathematical analysis (see Section VI.C) and MATLAB simulations that the presence of the series capacitor in the faulted phase did not affect the ringing frequency.

III. Algorithm Description

Much of the secondary arcing algorithm is similar to the algorithm presented in [1]. Therefore, the parts that are the same will be briefly mentioned in this section, with most of the focus on the advances made to the algorithm. More specifically, the magnitude comparator that relies on mutual coupling line parameters and the peak tracker supervision, which are now removed. Instead, a dc detection logic and a very-high magnitude check are added, as discussed in the following subsections.

A. DC Detection With CCVTs

As discussed in Section II.A, when the secondary arc extinguishes there will be a very slow decaying dc offset on the open-phase voltage, causing a CCVT transient. The dc detection logic detects the signatures of the CCVT transient response to this dc in the voltage signal.

The behavior of the CCVT when a dc offset is passed through it is shown in Fig. 2. Even though the CCVTs have different responses, both of them cause the voltage to be unidirectional for a much longer period than half of a power system cycle. This forms the basis of the first part of the dc detection logic, which looks for dc voltage (of either polarity) that exists for a duration longer than the dc counter threshold, as in Fig. 8a, leading to the assertion of DC_HI. The dc value is extracted from the raw open-phase voltage with the help of a low-pass filter, which removes the fundamental frequency and higher frequencies.

The removal of the primary fault via single-pole tripping (SPT) can lead to trapped energy in the CCVT, which then decays during the next few cycles after the single-pole opening of the breaker. This may be oscillatory in nature and can cause DC_HI to assert. Therefore, supervisory logic is used that requires a jump in the dc signal, as in Fig. 8b. For this logic, a two-cycle running peak tracks the energy inside the CCVT and the present dc value is required to be one and one half times the 5 ms old peak to assert DC_JUMP_DET. Because arcing is a random phenomena, it is possible to have multiple restrikes during the open interval period. Each of these may cause a new dc jump and also lead to extended dc voltage of both polarities. However, because this is arcing, it is characterized by high harmonics. Therefore, the DC_HI bit, supervised by DC_JUMP_DET, is used to start a delayed observation window during which, it is ensured that harmonics are not present before asserting DC_DET, which feeds into the SAED logic, as in Fig. 8c.

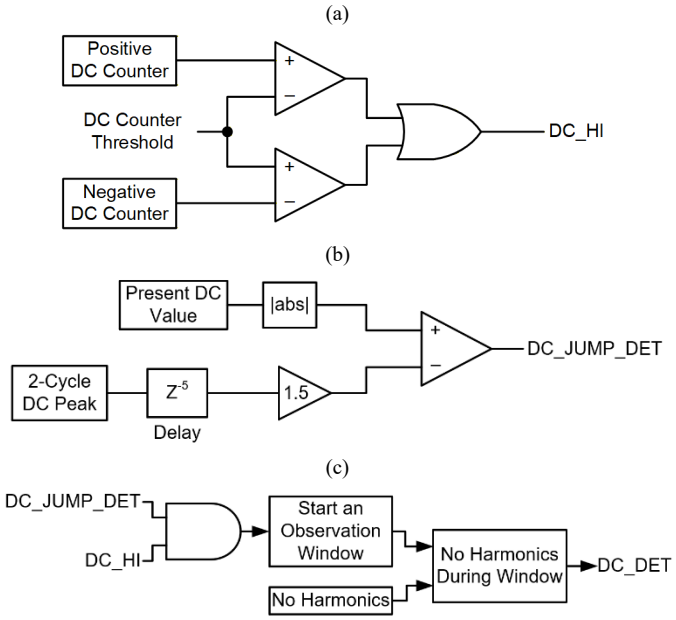

Fig. 8. DC detection logic.

B. SAED Detection Logic

In [1], two separate logic algorithms for SAED were proposed, which depended on whether the line was shunt reactor compensated or not. In this paper, these two pieces of logic have been combined, so that the algorithm now does not require a setting for the shunt-reactor-compensation status of the line. This is useful if a compensated line has its shunt reactors removed from service during high loading. The flow diagram of the entire algorithm is shown in Fig. 9.

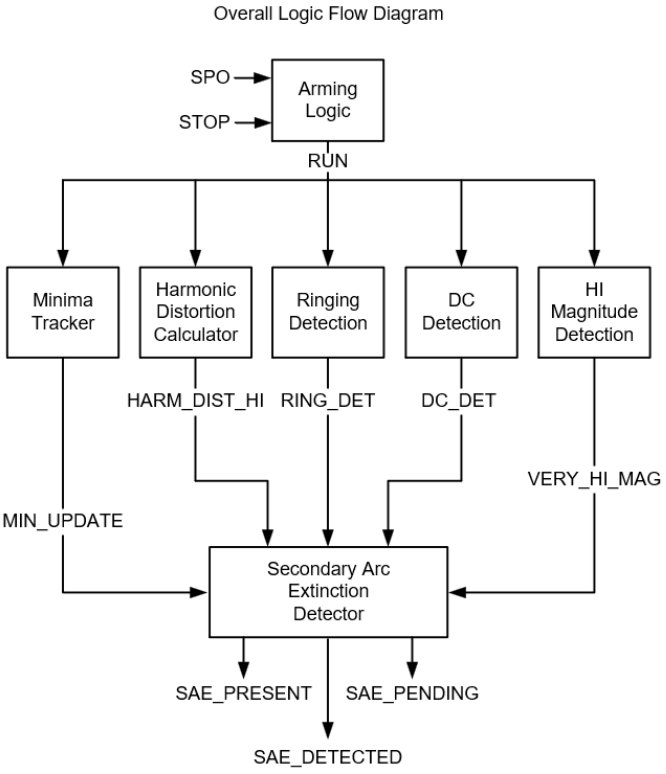

Fig. 9. Logic flow diagram for SAE detector.

The MIN_UPDATE and HARM_DIST_HI inputs come from the minima tracker and harmonic distortion calculation blocks, respectively, which are covered in [1]. Note that the peak tracker from [1] is no longer required with the new dc detection method for uncompensated lines. The intent of the minima tracker is to make sure that the phasor magnitude of the secondary voltage has fully dropped from the previous fault voltage value. The harmonic distortion calculator determines if the open-phase voltage contains a substantial amount of harmonics. If either of these two signals is asserted, it indicates that the secondary arc has not extinguished. Therefore, both of these conditions must be false for three cycles before the SAE_DETECTED can assert and the secondary arc can be declared extinguished.

When the recovery voltage of a compensated line with three reactors is greater than 90 percent of the nominal voltage, VERY_HI_MAG asserts. The high-magnitude check complements the ringing detection. For heavily compensated lines, the ringing frequency may be too close to the fundamental frequency (within 3 Hz) to distinguish between the two. In those cases, the high-magnitude recovery voltage produced by that level of compensation will assert VERY_HI_MAG and declare SAE_DETECTED.

Ringing detection, described in [1], is used to determine if an SAE has occurred on shunt-reactor-compensated lines, unless the reactor configuration and compensation level is such that the ringing frequency is too close to the nominal frequency. In this case, the very high-magnitude check is used. Ringing is enabled when harmonics are detected after the transients from the breaker opening have subsided. This prevents ringing from picking up due to the disturbance introduced when the primary fault is removed.

If the blocking signals (MIN_UPDATE and HARM_DIST_HI) have been deasserted for three cycles and any of the SAE signatures (VERY_HI_MAG, RING_DET, or DC_DET) assert, the SAE_DETECTED output asserts, indicating that the secondary arc has extinguished (see Fig. 10). The three-cycle time allows the dielectric strength to build sufficiently to withstand the full nominal voltage plus any reclosing transients before SAE_DETECTED is declared and the breaker is allowed to reclose [1] [3].

If the secondary arc extinguishes close to the end of the open interval, the three-cycle timer prevents SAE_DETECTED from asserting because the dielectric strength of the media may not have had enough time to recover in order to withstand full nominal voltage plus reclosing transients. The SAED_PENDING output indicates that the secondary arc extinction was detected, but it was too close to the end of the open interval time for SAE_DETECTED to assert. A short delay past the open interval time could be applied for successful single-pole reclosing in this scenario.

The secondary arcing present logic is also shown in Fig. 10. This logic is very similar to the block reclose logic presented in [1]. The High-Magnitude Check, Ringing Detected, and DC Detected signals into the NOR gate replace the Compensated Magnitude Threshold Check or Ringing Detected in the previous two separate block-reclose logics. The logic also requires that harmonics are high AND that there is an absence of any positive indicators of the SAE.

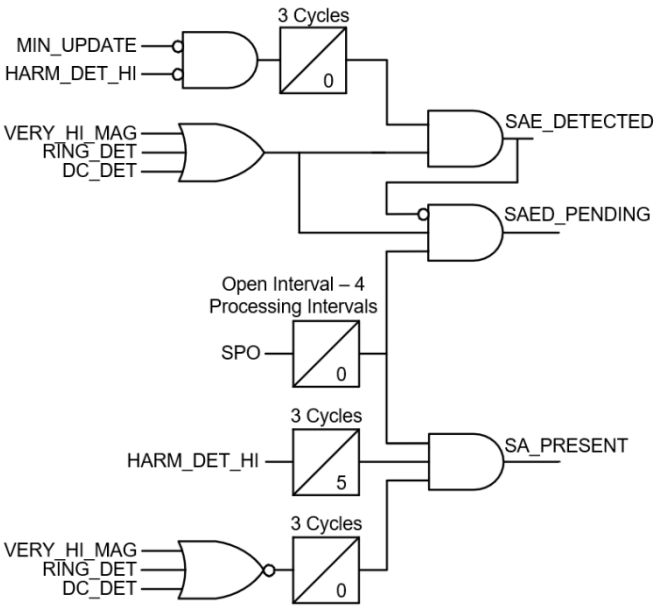

Fig. 10. SAE detection logic.

There are three explicit outputs of the algorithm, SAE_DETECTED, SAED_PENDING, and SA_PRESENT. The SAE_DETECTED output indicates that the secondary arc existed on the open phase and extinguished with time for the dielectric to build up to withstand nominal voltage plus reclosing transients. The SAED_PENDING output indicates that the secondary arc extinction was detected; however, it was too close to the end of the open interval time for SAE_DETECTED to assert. The SA_PRESENT output indicates that arcing is still present at the end of the open interval and that if the single phase is reclosed, it will reignite the primary fault. If neither of these three outputs assert, then that implies a “no call” scenario, where the presence or absence of the secondary arc could not be determined.

There are two situations in which a “no call” scenario may occur. On lines without shunt compensation, if the arc extinguishes with the breaker opening or shortly thereafter, a “no call” may occur. This is not the case on lines with shunt compensation where the ringing persists for a longer period after the arc extinction. Bolted faults that do not arc or create harmonics will also result in a “no call” output because there is no arc or arc extinction to detect. In these “no call” scenarios, the scheduled reclose could continue or given the relatively low probability of very fast arc extinction on uncompensated lines, the “no call” output could be treated like the SA_PRESENT output and used to convert to three-pole trip.

IV. Simulation and Field Results

To test the functionality of the algorithm, the authors performed a combination of electromagnetic transient (using Electromagnetic Transients Program [EMTP]) simulations, in addition to the use of field cases that were provided from single-pole trip applications.

A. Simulation Results

EMTP models were built using the Real Time Digital Simulator (RTDS®). These systems were modeled using 500 kV transmission lines with the following configurations:

- Transposed, series compensated without shunt reactor compensation.
- Transposed, series compensated with four-legged reactor shunt compensation.
- Transposed, series compensated with three-legged reactor shunt compensation.

The primary fault was simulated as a bolted fault, whereas the fault during the open-pole condition was either simulated as a bolted fault to represent a permanent fault or as an arcing fault to represent a temporary fault that clears before the pole-open interval time expires (dead time). A secondary arc model was used, as in [8], with varying arc duration and reignition to model the arc during the open-pole condition. The RTDS model also included the built-in CCVT to measure the voltage signals. Furthermore, two additional CCVT models (the same ones used in generating Fig. 2; refer to Section VI.A for more details) were used in this study to evaluate the impact of different types of CCVT on the algorithm. The simulation results included in this paper show only the RTDS CCVT output for clarity; however, the algorithm response with the other CCVT models was similar. Common Format for Transient Data Exchange (COMTRADE) files were generated that contained the raw voltages, currents, and breaker status for each case. The raw voltages were filtered and resampled in MATLAB and fed to the algorithm to validate its performance. The simulation results for each configuration and fault type (permanent and temporary) follow.

1) *Transposed Series-Compensated Line Without Shunt Reactor Compensation*

The simulated system consists of a 134.9-mile, 500 kV transposed transmission line with series capacitors at both ends of the line compensating for 65 percent of the line. The faults are simulated at 47 percent of the line length from the local end.

Consider the case of a temporary fault in which the secondary arc extinguishes before the end of the dead time. In Fig. 11, the first plot shows the raw faulted phase voltage as measured by the CCVT. Notice that the dc offset is not visible at SAE because the CCVT removes it. Only the dc transient remains, which is shown in the second plot. The third plot shows the cumulative root-mean-square (rms) sum of the second through fifth harmonics and the threshold to which it is compared. The final plot shows all digitals related to the algorithm.

As shown in the first plot, the primary fault starts at 0.08 s and the faulted phase pole opens at 0.13 s, after which the secondary arc is established. During this secondary arcing period, the distortion in the raw voltage is evident and can also be seen from elevated harmonics. The SAE occurs at 0.55 s, at which point the voltage becomes clean. At SAE, a positive surge in the dc is seen and then a negative dc with a long decay, leading to a DC_DET assertion after a delayed observation window during which no harmonics are seen (refer to Section III.A). This also asserts the SAE_DETECTED output, which can be used to speed up reclosing. In this simulated event, a dead time of 1.14 s was used, and the faulted phase successfully reclosed at 1.27 s. Given that SAE_DETECTED asserted at 0.62 s, the reclose could have been achieved 0.64 s sooner, subject to the breaker minimum duty cycle time. Alternatively, this can also be used as confirmation that the secondary arc (SA) has extinguished to supervise the reclose.

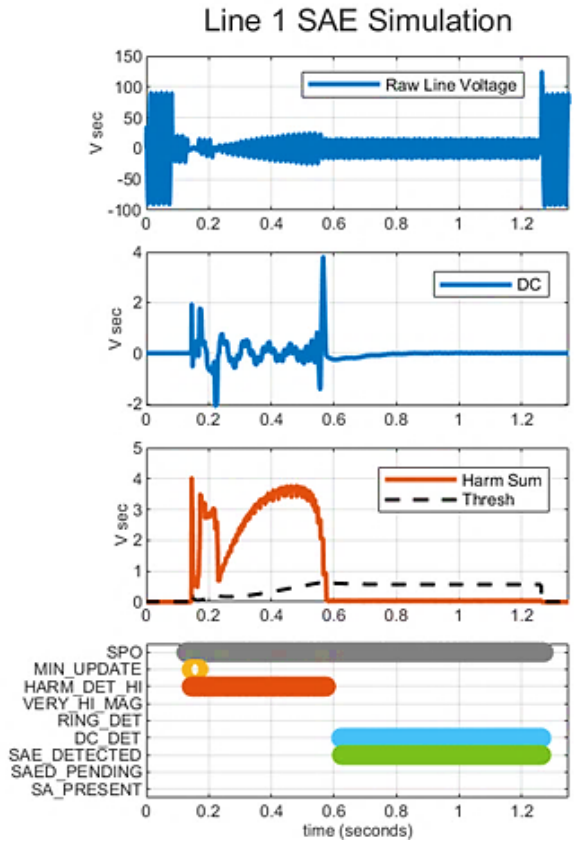

Fig. 11. Arc extinction on a series-compensated line.

Next, consider the case of a permanent bolted fault for the same line and at the same fault location. As shown in Fig. 12, the primary fault starts at 0.08 s and is isolated at 0.13 s. An initial surge in the harmonics is indeed seen; however, this is mostly due to phasor transients, after which the harmonic activity is absent. The dc shows the low-frequency oscillations (i.e., approximately 13.7 Hz) coming from the CCVT due to it containing trapped energy. However, this transient is decaying in nature and a new surge in dc is not seen, which is required to assert DC_DET. Because none of the SAE conditions are seen by the end of the dead time, SA_PRESENT asserts a few processing intervals before the end of the dead time and can be used to block the reclose. Note that in this event, a shorter dead time of 0.8 s was used.

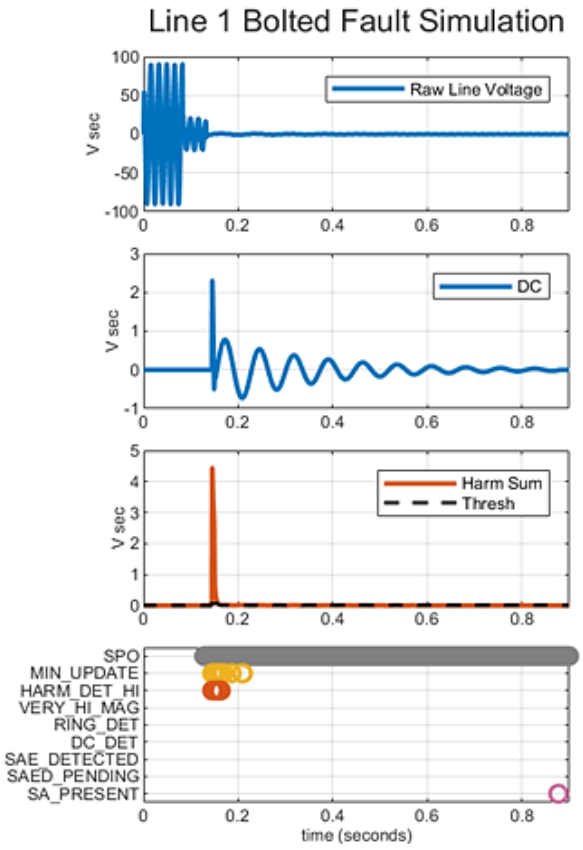

Fig. 12. Permanent bolted fault on a series-compensated line.

2) Transposed Series-Compensated Line With Four-Legged Reactor Shunt Compensation

The simulated system consists of a 134.9-mile, 500 kV transposed transmission line with series capacitors at both ends of the line compensating for 65 percent of the line and four-legged shunt reactors at the local end of the line compensating for 50 percent of the line susceptance. The faults are simulated at 47 percent of the line length from the local end.

Consider the case of a temporary fault in which the secondary arc extinguishes before the end of the dead time. In Fig. 13, the second plot shows the phasor magnitude, the mean magnitude, and the ringing magnitude. Note that the mean magnitude represents the true fundamental frequency magnitude and it removes the impact of the ringing frequency component.

The distortion in the phasor magnitude indicates that the primary fault starts at 0.09 s and the faulted phase breaker opens at 0.13 s, at which point the secondary arc is established. During this time, the distortion in the raw voltage is evident and can also be seen from the elevated harmonics. The SAE occurs at 0.43 s, at which point the ringing is evident from the complementary frequency oscillation in the phasor magnitude. This complementary frequency is approximately 20 Hz, which indicates a ringing frequency of 40 Hz (i.e., equals 60 Hz–20 Hz) corresponding to a percentage shunt compensation of approximately 50 percent. The presence of ringing is detected by the algorithm and RING_DET asserts. This also leads to a dynamic adjustment in the harmonic threshold, which uses the ringing magnitude to account for leakage of the ringing component into the harmonics measurement. This resets the HARM_HI bit and leads to the SAE_DETECTED assertion, which can be used to speed up reclosing. In this simulated event, a dead time of 1.15 s was used, and the faulted phase successfully reclosed at 1.28 s. Given that SAE_DETECTED asserted at 0.56 s, the reclose could have been achieved 0.72 s sooner, subject to the breaker minimum duty cycle time, which is a significant time savings on a dead time of 1.15 s. Alternatively, this can also be used as confirmation that the SA has extinguished to supervise the reclose.

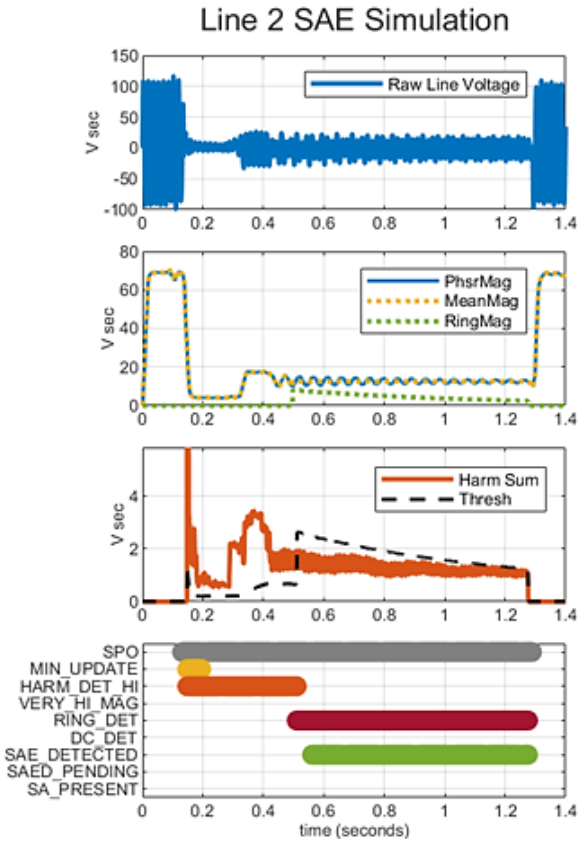

Fig. 13. Arc extinction on a series- and shunt-compensated line.

Next, consider the case of a permanent bolted fault for the same line and at the same fault location. In Fig. 14, the primary fault starts at 0.09 s and is isolated at 0.14 s. The harmonic activity is absent after the initial few cycles. There is no sign of ringing by the end of dead time, at which point the SA_PRESENT asserts, which can be used to block the reclose. Note that in this event, a shorter dead time of 0.8 s was used.

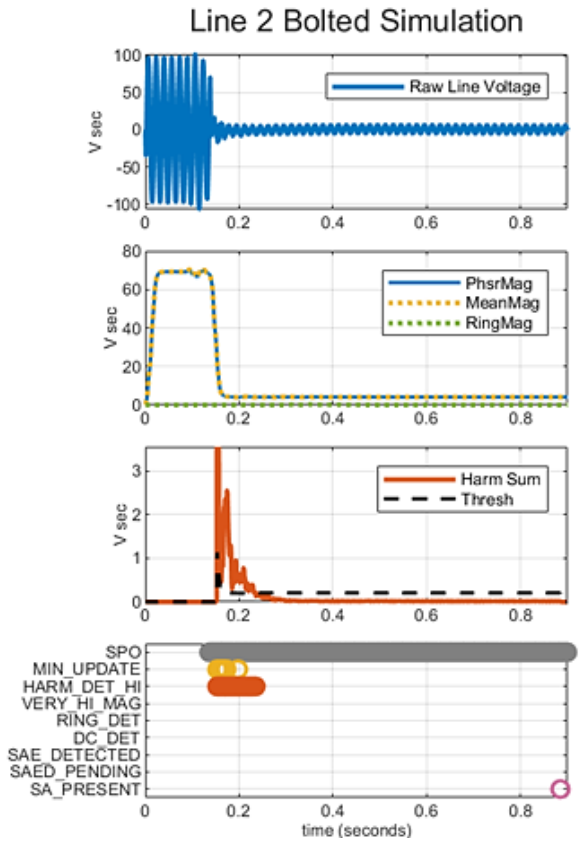

Fig. 14. Permanent bolted fault on a series- and shunt-compensated line.

3) *Transposed Series-Compensated Line With Three-Legged Reactor Shunt Compensation*

The simulated system consists of a 134.9-mile, 500 kV transposed transmission line with series capacitors at both ends of the line compensating for 65 percent of the line and three-legged shunt reactors at the local end of the line compensating for 96 percent of the line susceptance. The authors intentionally chose this high degree of compensation to highlight how, in certain cases, ringing frequency can get very close to the nominal frequency and the voltage magnitude can become extremely high. The faults are simulated at 47 percent of the line length from the local end.

Consider the case of a temporary fault in which the secondary arc extinguishes before the end of the dead time. For this event, a dead time of 1.15 s was used. In Fig. 15, the second plot shows the phasor magnitude, the mean magnitude, and the ringing magnitude.

Though not evident, it can be seen from the distortion in the phasor magnitude that the primary fault starts at 0.08 s and the faulted phase breaker opens at 0.13 s, after which the secondary arc is established. During this secondary arcing period, the open-phase voltage magnitude is very low (i.e., approximately 5 percent of nominal voltage). The harmonics are elevated during this time. The SAE occurs at 0.35 s, at which point the voltage magnitude rises sharply. The voltage magnitude crosses the very high-magnitude threshold of 90 percent of nominal voltage at 0.39 s, at which point VERY_HI_MAG asserts and causes SAE_DETECTED to assert after some qualifying time delay. The voltage magnitude keeps rising to greater than 300 percent of the nominal voltage. The percentage shunt compensation in this case is 96 percent, which is higher than the compensation level at which the voltage magnitude asymptotes (i.e., 88 percent) for a line with C_0/C_1 of 0.64 (C_M/C_S of 0.14), which is the ratio in this case (see Section II.D). Some ringing is present in the raw voltages and phasor magnitude; however, this ringing frequency is close to nominal. As the compensation decreases, initially the voltage magnitude increases (i.e., to a maximum at 88 percent compensation) and then decreases. At some point, the voltage magnitude will go below the high-magnitude threshold; however, before that point, the ringing frequency will be in the tracking range and ringing will be detected for those cases. For this event, the reclose could have been achieved 0.89 s sooner, subject to the breaker minimum duty cycle time, which represents a significant time savings on a dead time of 1.15 s. Alternatively, this can be used as confirmation that SA has extinguished to supervise the reclose.

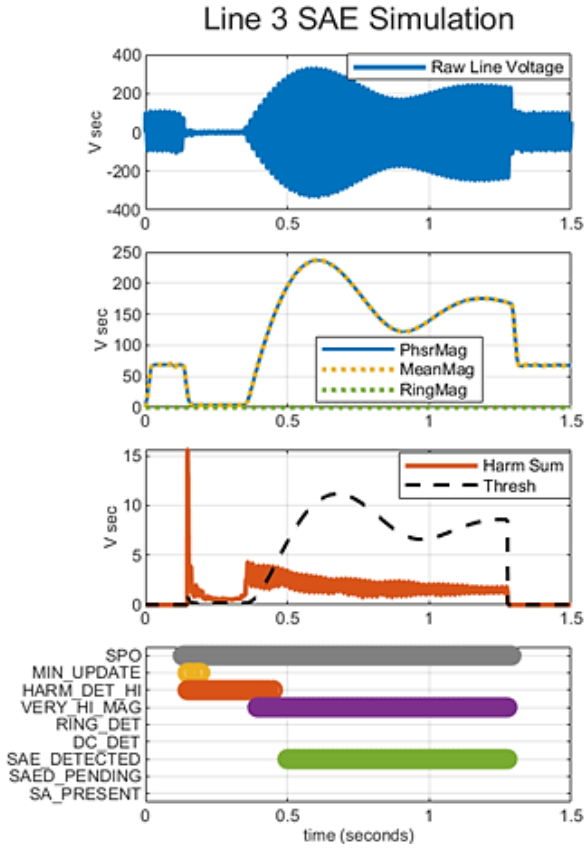

Fig. 15. Arc extinction in a transmission line with grounded three-legged shunt reactors.

Next, consider the case of a permanent bolted fault for the same line and at the same fault location. The percentage shunt compensation in this case is 50 percent. In Fig. 16, the primary fault starts at 0.09 s and is isolated at 0.17 s. The harmonic activity is erratic, and it disappears after initial assertion. The voltage magnitude remains low by the end of the dead time, at which point the SA_PRESENT asserts, which can be used to block the reclose. Note that in this event, a shorter dead time of 0.8 s was used.

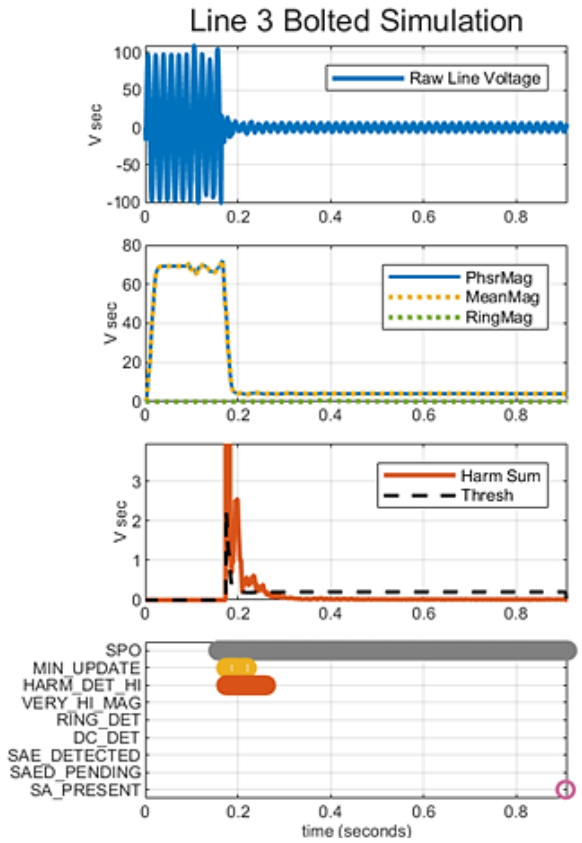

Fig. 16. Permanent fault in a transmission line with grounded three-legged shunt reactors.

B. *Field Events*

In this section, the performance of the proposed algorithm is analyzed for three field events. The first event is an arc extinction on an uncompensated, parallel line. The second event is an arc extinction on a four-legged reactor shunt-compensated, parallel line. The last event is a permanent fault on the same line as the second event.

For each event, raw voltages are extracted from COMTRADE files that were collected from relays protecting the line. The raw voltages are preprocessed to resample them for the algorithm processing rate, track the fundamental frequency, and calculate the phasors at the fundamental and second through fifth harmonics. The preprocessed values are fed into the algorithm to validate its performance.

These field events are the same events evaluated in [1]. The updated algorithm performance is validated for correct operation and compared with the prior version of the algorithm.

1) *Field Event 1: Arc Extinction on an Uncompensated, Transposed, Parallel Line*

This event is a Phase B-to-ground fault on a 60 Hz, 230 kV, 162.4 km parallel line without shunt reactor compensation. The relay reported the fault location as 30.3 km [1].

The first (upper) plot in Fig. 17 shows the raw Phase B voltage. The fault occurs 0.09 s into the event and the faulted phase is isolated at 0.4 s. After isolation, the secondary arc persists until 0.43 s. At 0.67 s, the remote end closes (dead time of 30 cycles) and successfully re-energizes the line.

The second plot in Fig. 17 shows the dc extracted from the Phase B voltage. During the arcing period, the dc component appears randomly distributed around zero. When the arc extinguishes, the CCVT transient response to the decaying dc offset is evident.

The third plot in Fig. 17 shows the calculated harmonic distortion and the harmonic detection threshold. Reference [1] includes a detailed explanation of the harmonic filtering and the adaptive threshold logic, which is unchanged in the updated algorithm. Harmonic distortion is elevated during the arcing period and drops significantly after the arc extinguishes. During the arcing period, the threshold increases as the open-phase voltage magnitude increases.

The fourth (lower) plot in Fig. 17 shows the algorithm outputs. Shortly after the SPO condition occurs, the minima tracker (MIN_UPDATE) asserts and does not assert again for the rest of the event. The harmonic detection (HARM_DET_HI) is asserted throughout the arcing period and deasserts when the arc extinguishes. The high-magnitude check (VERY_HI_MAG) and ringing detection (RING_DET) remain deasserted throughout the event, as expected for an uncompensated line. After the arc extinguishes, the dc jump logic is triggered by the CCVT transient response and the dc observation window is started. At the end of the observation window, the dc counter threshold is exceeded, and the dc detection output (DC_DET) asserts at 0.50 s. Because the dc detection asserts and all blocking conditions are deasserted, the SAED output (SAE_DETECTED) asserts. The SAED pending (SAED_PENDING) and arcing present (SA_PRESENT) outputs do not assert.

The SAED output can be used for reclosure supervision at the end of the dead time. Alternatively, it can be used to initiate reclose prior to the end of the dead time. In this event, initiating reclose on the assertion of the SAED output would result in re-energizing the line 0.17 s sooner, subject to the breaker minimum duty cycle time.

2) Field Event 2: Arc Extinction on a Compensated, Transposed, Parallel Line

This event is a Phase A-to-ground fault on a 60 Hz, 230 kV, 145 km parallel line with four-legged shunt reactor compensation on one end of the line. The relay reported the fault location as 96.76 km [1].

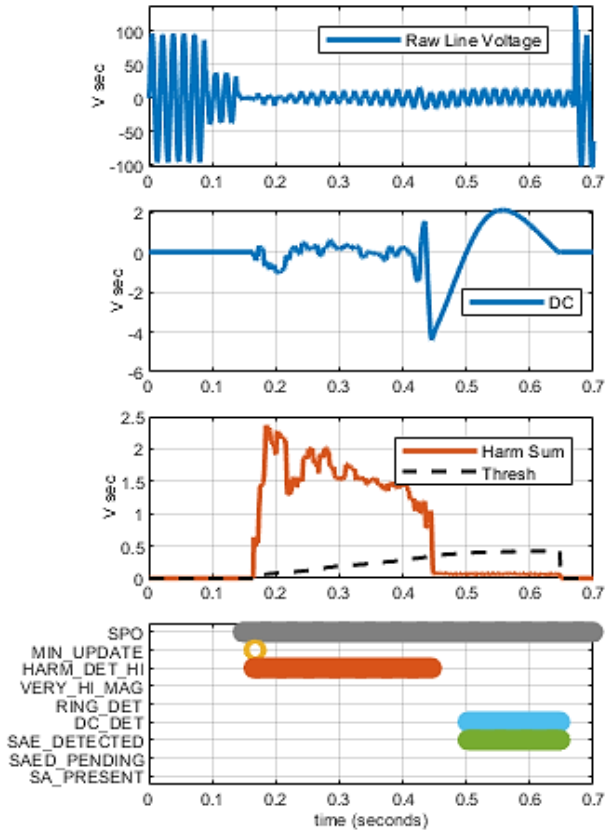

Fig. 17. Field Event 1: Arc extinction on uncompensated line.

The first plot in Fig. 18 shows the raw Phase A voltage. The fault occurs 0.49 s into the event, and the faulted phase is isolated at 0.55 s. After isolation, there is a short period of high-frequency transients and the secondary arc persists until approximately 0.64 s, after which ringing is evident. At 1.08 s the remote end closes (dead time of 30 cycles) and successfully re-energizes the line.

The second plot in Fig. 18 shows the open-phase voltage phasor magnitude, mean (fundamental) phasor magnitude, and ringing phasor magnitude. Reference [1] includes a detailed explanation of the filtering for extraction of these signals, which is unchanged in the updated algorithm. After isolation, the phasor magnitude oscillates; initially due to high-frequency transients and then due to the ringing from the arc extinction. The mean magnitude tracks the phasor magnitude until ringing is detected, at which point the filtering removes the ringing frequency oscillations and the mean tracks only the fundamental component of the open-phase voltage. The ringing magnitude is zero until ringing is detected, after which it tracks the magnitude of the ringing component of the open-phase voltage.

The third plot in Fig. 18 shows the calculated harmonic distortion and the harmonic detection threshold. Harmonic distortion is highly elevated during the high-frequency transient and arcing periods and then decreases after the arc extinguishes. Because of leakage from the ringing, the harmonic distortion remains slightly elevated after arc extinction. Once ringing is detected and qualified, it is removed from the phasor magnitude (approximately one beat frequency cycle after the first frequency measurement). The mean magnitude and the measured ringing frequency are then used to raise the adaptive harmonic threshold to account for the ringing leakage.

The fourth plot in Fig. 18 shows the algorithm outputs. Shortly after the SPO condition occurs, the minima tracker (MIN_UPDATE) asserts. It asserts again when the arc extinguishes and then does not assert for the rest of the event. The harmonic detection (HARM_DET_HI) is asserted until ringing is detected, and the adaptive threshold is raised. The high-magnitude check (VERY_HI_MAG) remains deasserted throughout the event, as expected for a line that is not heavily compensated by a three-legged reactor. The dc detection output (DC_DET) also remains deasserted throughout the event. After the arc extinguishes, ringing detection (RING_DET) asserts at 0.72 s. Because ringing detection is asserted and all blocking conditions are deasserted, the SAED output (SAE_DETECTED) asserts at 0.81 s. The SAED pending (SAED_PENDING) and arcing present (SA_PRESENT) outputs do not assert.

In this event, initiating reclose on the assertion of the SAED output would result in re-energizing the line 0.27 s sooner, subject to the breaker minimum duty cycle time.

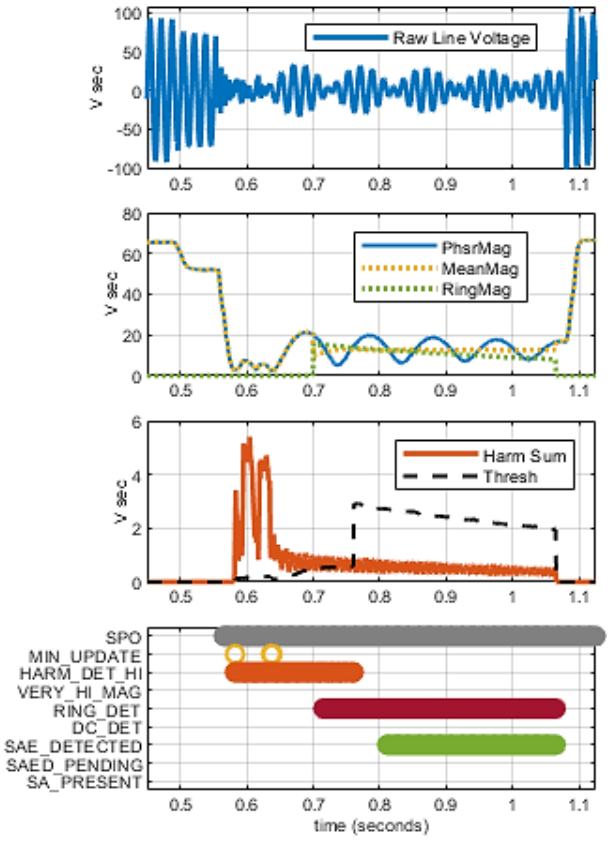

Fig. 18. Field Event 2: Arc extinction on four-legged shunt-reactor-compensated line.

3) Field Event 3: Permanent Fault on a Compensated, Transposed, Parallel Line

This event is a Phase B-to-ground fault on the same line as Field Event 2. The relay reported the fault location as 56.82 km [1].

The first plot in Fig. 19 shows the raw Phase B voltage. The fault occurs at 0.49 s into the event, and the faulted phase is isolated at 0.55 s. After isolation, there is a short period of high-frequency transients followed by an extended period of low amplitude with little distortion and no ringing. At 1.09 s (dead time of 30 cycles), the remote end unsuccessfully attempts to re-energize the line.

The second plot in Fig. 19 shows the open-phase voltage phasor magnitude, mean (fundamental) phasor magnitude, and ringing phasor magnitude. After isolation, the phasor magnitude remains very low. The mean magnitude tracks the phasor magnitude throughout because ringing is not detected. Likewise, the ringing magnitude is zero throughout the event.

The third plot in Fig. 19 shows the calculated harmonic distortion and the harmonic detection threshold. Harmonic distortion is highly elevated during the high-frequency transient period and then decreases significantly and remains near the threshold level throughout the remainder of the event. Because ringing is not detected and the phasor magnitude remains low, the harmonic threshold is relatively constant throughout the event.

The fourth plot in Fig. 19 shows the algorithm outputs. Shortly after the SPO condition occurs, the minima tracker (MIN_UPDATE) asserts intermittently for a few cycles and then does not assert again for the rest of the event. The harmonic detection (HARM_DET_HI) asserts intermittently throughout the entire event and the harmonic distortion hovers near the threshold level. The high-magnitude check (VERY_HI_MAG), ringing detection (RING_DET), and dc detection (DC_DET) all remain deasserted throughout the entire event, which is expected for a permanent fault. Because neither high magnitude, ringing, nor dc are detected and the harmonic detection continues to assert, the SAED output (SAE_DETECTED) does not assert, nor does the SAED pending (SAED_PENDING) output. At two processing intervals before the end of the dead time, the arcing present output (SA_PRESENT) does assert.

In this event, the assertion of the SA_PRESENT output could be used to prevent the reclose attempt and convert to a three-pole trip.

4) Comparison With the Previous Algorithm

In all three field events, the updated algorithm compares well to the previous version. For Field Event 1, the new dc detection algorithm is slightly slower in detecting the arc extinction; however, it still asserts well before the end of the dead time. The new algorithm, however, does not require any line parameters for the parallel line to successfully detect SAED. For Field Event 2, although the ringing detection algorithm is largely unchanged in the new algorithm, the SAED output is slightly slower due to additional security enhancements. As with Field Event 1, it still asserts well before the end of the dead time. For Field Event 3, the operation is identical and the updated algorithm correctly asserts the arcing present output at the end of the dead time.

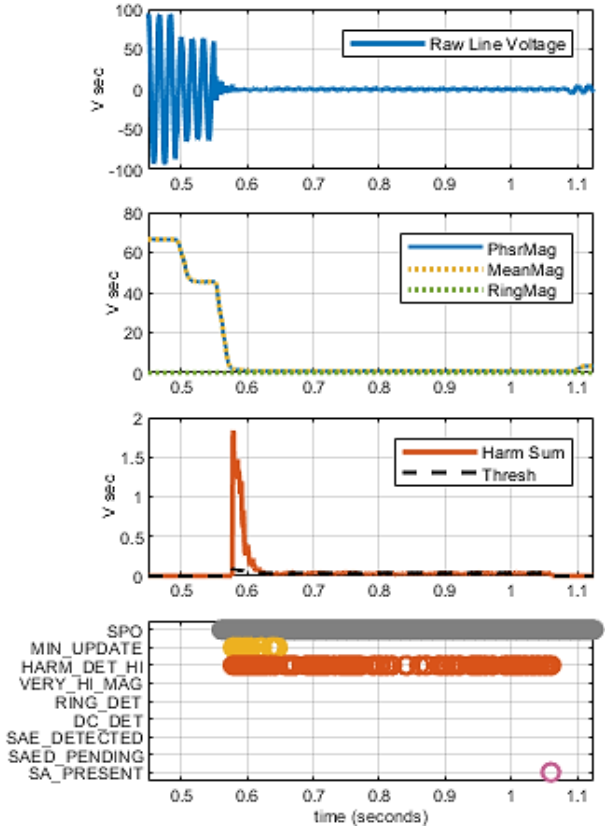

Fig. 19. Field Event 3: Permanent fault on four-legged shunt-reactor-compensated line.

V. Conclusion

Single-pole tripping and reclosing is used to maintain power transfer and system stability when clearing single-line-to-ground faults. However, coupling between the open phase and the healthy phases and possibly with the parallel lines, can sustain the primary fault arc, causing a secondary arc. An adaptive reclosing scheme that detects the extinction of the secondary arc can improve system stability by allowing the reclose to occur sooner or by preventing a reclose onto a fault when the arc has not extinguished.

In [1], the authors proposed an algorithm to detect SAEs. That algorithm was developed for transmission lines without shunt reactor compensation and lines with four-legged shunt reactor compensation. It did not consider transmission lines compensated with three-legged shunt reactors or series-compensated lines. The algorithm required knowledge of whether the protected line was shunt compensated to engage the appropriate detection method. Additionally, the method for uncompensated lines required mutual admittance parameters that can be difficult to obtain for parallel lines. This paper extends the algorithm proposed in [1] to accommodate three-legged shunt-reactor-compensated lines and series-compensated lines, and to remove settings for additional system information.

As described in this paper, for lines without shunt compensation, an extended dc detector replaces the previous

compensated voltage magnitude method. The new method does not require mutual line admittances or measurements from parallel lines. Instead, it relies on identifying the transient response of the open-phase CCVT to the decaying dc voltage produced by the arc extinction.

For four-legged shunt-reactor-compensated lines, the algorithm remains largely unchanged. It detects and measures the ringing frequency after arc extinction, both as a positive indication of arc extinction and to boost the harmonic detection threshold to prevent incorrect blocking because of harmonic filter response to the ringing frequency.

For three-legged shunt-reactor-compensated lines, analysis and simulation demonstrate that the ringing detection is still effective, except when the level of compensation pushes the ringing frequency close to the fundamental. However, in those cases, a simple high-set magnitude check can substitute for the ringing detection.

For series-compensated lines, both with and without shunt reactor compensation, analysis and simulation demonstrates that both the ringing detection and dc detection methods are effective.

These three methods of dc detection, ringing detection, and the very high-magnitude check for secondary arc extinction detection are combined in simple logic that runs during the single-pole open condition, after a short qualifying delay. All three positive indicators are always active. This is especially useful considering that shunt compensation can be dynamically switched, based on loading conditions. The three methods are supervised by the absence of high-harmonic distortion. If any of the three SAE detectors asserts and harmonics have been below threshold for at least three cycles, the algorithm asserts the SAE detected output. This output can be used to supervise reclosing at the end of the dead time or to initiate early reclosing before the end of the dead time. Alternatively, if none of the SAE detectors asserts and harmonics have been above threshold for three cycles, the algorithm asserts the arcing present output at the end of the dead time. The arcing present output can be used to prevent reclosing onto a persistent fault and to convert it to a three-pole trip.

The updated algorithm was validated against EMTP simulations and the same field cases that were presented in [1]. In all situations, it either correctly blocked reclosing or identified the arc extinction.

VI. Appendix

A. CCVT Verification

Two CCVT models, CCVT1 and CCVT4, were considered from [5]. The CCVTs were modeled using MATLAB and Simulink with the parameter values provided in the paper. The Frequency Response Estimator (FRE) block was used to estimate the frequency response of the CCVTs and match it with the frequency response provided in [5]. These two CCVTs (CCVT1 and CCVT4) were also used in this paper. Note that because only two of the CCVTs were used, the CCVT2 reference in this paper is CCVT4 in [5].

B. Ringing Frequency and Open-Phase Voltage Magnitude on Three-Reactor-Compensated Line

1) Ringing Frequency

From Fig. 4:

$$\omega_{RING} = \frac{1}{\sqrt{L_P \bullet C_S}} \tag{5}$$

$$f_{RING} = \frac{1}{2 \bullet \pi} \frac{1}{\sqrt{L_P \bullet C_S}} \tag{6}$$

where:

$$L_P = \frac{1}{\omega^2 \bullet Comp_{PU} \bullet C_1} \tag{7}$$

$$C_1 = C_S + C_M \tag{8}$$

Substituting (7) and (8) into (6):

$$f_{RING} = \frac{1}{2\pi} \frac{1}{\sqrt{\frac{C_S}{\omega^2 \bullet Comp_{PU} \bullet (C_S + C_M)}}} \tag{9}$$

$$\Rightarrow f_{RING} = \frac{\omega}{2\pi} \sqrt{Comp_{PU} \bullet \left(1 + \frac{C_M}{C_S}\right)} \tag{10}$$

$$\Rightarrow f_{RING} = f_{NOM} \sqrt{Comp_{PU} \bullet \left(1 + \frac{C_M}{C_S}\right)} \tag{11}$$

$$\Rightarrow f_{RING\_PU} = \frac{f_{RING}}{f_{NOM}} \sqrt{Comp_{PU} \bullet \left(1 + \frac{C_M}{C_S}\right)} \tag{12}$$

2) Open-Phase Voltage Magnitude

From Fig. 5b, we have a generic voltage divider as shown in (13).

$$V_{Opn} = V_{AVG} \bullet \left(\frac{Z_2}{Z_1 + Z_2}\right) = V_{AVG} \bullet \left(\frac{Y_1}{Y_1 + Y_2}\right) \tag{13}$$

where:

Z_1 is the impedance of $2C_M$.

Z_2 is the impedance of the parallel combination of C_G and L_P.

Substituting the appropriate values we get:

$$V_{Opn} = V_{AVG} \bullet \left(\frac{j\omega(2C_M)}{j\omega(2C_M) + j\omega(C_G) + \frac{1}{j\omega L_P}}\right) \tag{14}$$

Substituting L_P from (7) and using (8), in addition to using the fact that $2C_M + C_G = C_S$, we get:

$$V_{Opn} = V_{AVG} \bullet \left(\frac{j\omega(2C_M)}{j\omega(C_S) + \frac{\omega^2 Comp_{PU}(C_S + C_M)}{j\omega}}\right) \tag{15}$$

$$V_{Opn} = V_{AVG} \bullet \left(\frac{j\omega(2C_M)}{j\omega(C_S) - j\omega Comp_{PU}(C_S + C_M)} \right) \quad (16)$$

$$\Rightarrow V_{Opn} = V_{AVG} \bullet \left(\frac{2C_M}{C_S - Comp_{PU}(C_S + C_M)} \right) \quad (17)$$

$$\Rightarrow V_{Opn} = V_{AVG} \bullet \left(\frac{\frac{2C_M}{C_S}}{1 - Comp_{PU}\left(1 + \frac{C_M}{C_S}\right)} \right) \quad (18)$$

Note that V_{AVG} is $V_{NomLN}/2$, then we get:

$$V_{Opn\_PU} = \frac{V_{Opn}}{V_{AVG}} = \left(\frac{\frac{C_M}{C_S}}{1 - Comp_{PU}\left(1 + \frac{C_M}{C_S}\right)} \right) \quad (19)$$

C. *Impact of Series Capacitor on Ringing Shunt-Reactor-Compensated Line*

The three-phase transmission line circuit, shown in Fig. 20, is used for ringing analysis. The transmission line includes a series capacitor and four-legged shunt reactors on both ends of the line. The line resistance is assumed to be zero for simplicity. The faulted phase (Phase A) is isolated following the single-pole opening of line breakers at both ends. To analyze ringing, the fundamental frequency sources must be removed. Then shorting out the Phase B and Phase C voltages and simplifying the circuit a bit, the result is shown in Fig. 21. Simplifying the circuit further, recall that $C_S = C_G + 2C_M$ and also define $L_X = L_P + \frac{L_P \parallel 2L_N}{2}$. Lastly, the subsynchronous oscillation occurs when the arc extinguishes; therefore, R_{ARC} is also removed from the circuit. After these simplifications, the resulting figure is shown in Fig. 22.

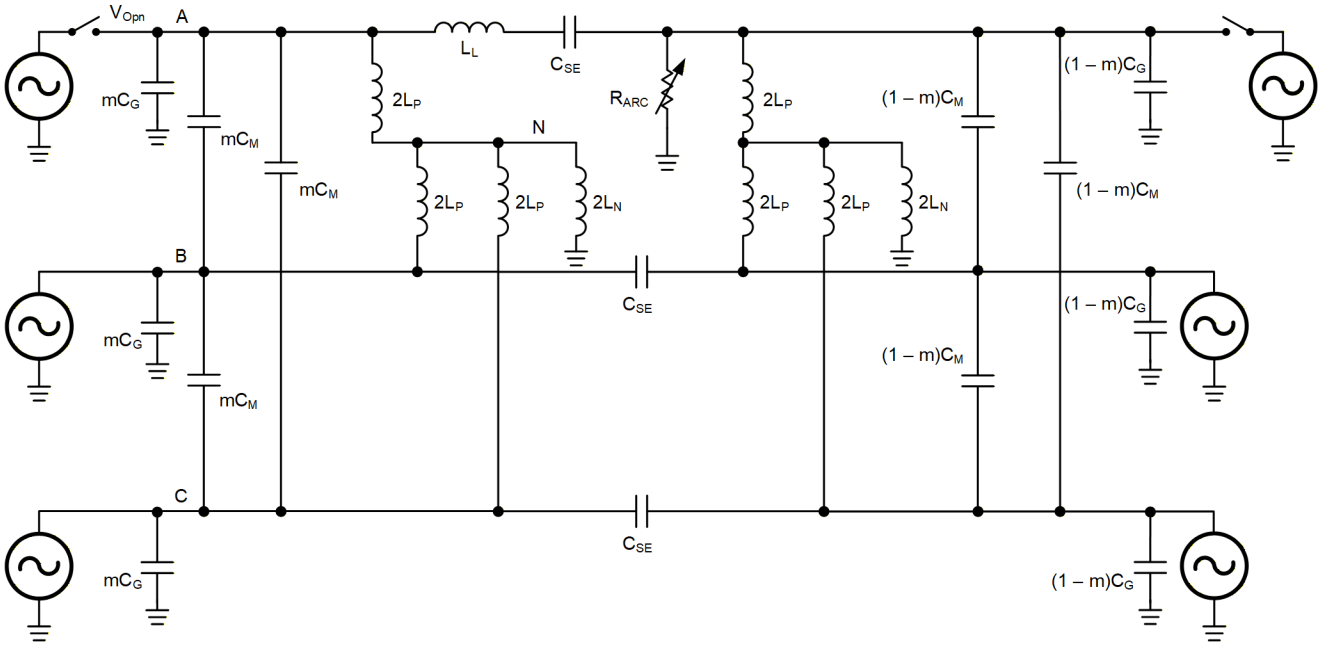

Fig. 20. Transmission line with series capacitor and four-legged shunt reactor bank on both ends.

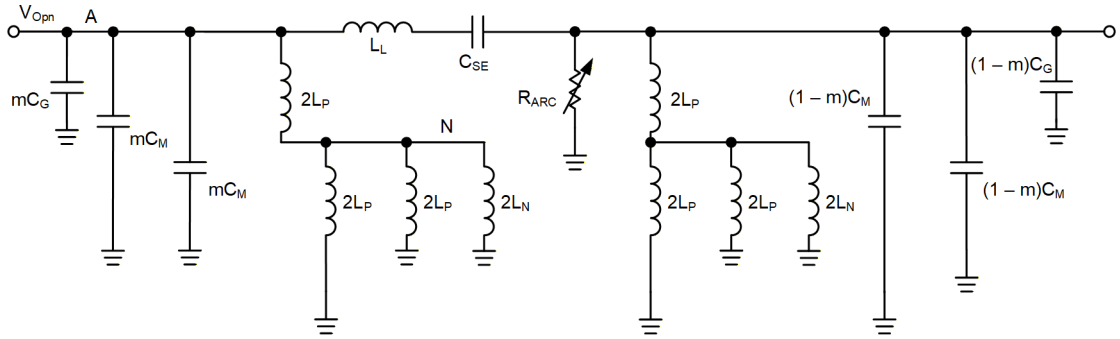

Fig. 21. Sources shorted and circuit simplified.

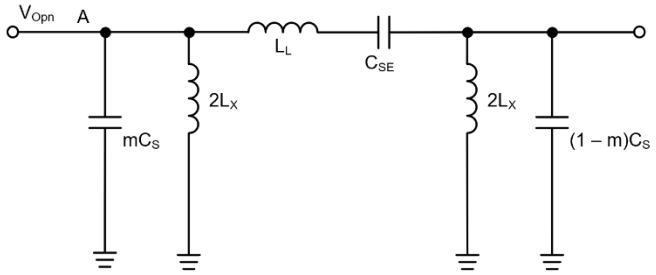

Fig. 22. Simplified circuit for ringing analysis.

$$Z_{eq}=\left(\frac{\left(\frac{1}{msC_S}\right)(2sL_X)}{\left(\frac{1}{msC_S}\right)+(2sL_X)}\right)\left\|\left(sL_L+\frac{1}{sC_{SE}}+\frac{\left(\frac{1}{m'sC_S}\right)(2sL_X)}{\left(\frac{1}{m'sC_S}\right)+(2sL_X)}\right)\right. \tag{20}$$

where:

$m' = 1 - m$.

$$z_{eq}=\frac{2sL_X\left[s^4\left(2m'C_{SE}L_LC_SL_X\right)+s^2\left(C_{SE}L_L+2L_XC_{SE}+2m'C_SL_X\right)+1\right]}{2s^2L\_XC_{SE}\left(s^2\left(2m'C_SL_X\right)+1\right)+\left(s^2\left(2mC_SL_X\right)+1\right)\left(s^4\left(2m'C_{SE}L_LC_SL_X\right)+s^2\left(C_{SE}L_L+2L_XC_{SE}+2m'C_SL_X\right)+1\right)} \tag{21}$$

$$\begin{aligned}&2s^2L_XC_{SE}\left(s^2\left(2m'C_sL_X\right)+1\right)+\left(s^2\left(2mC_SL_X\right)+1\right)\bullet\\&\left(s^4\left(2m'C_{SE}L_LC_SL_X\right)+s^2\left(C_{SE}L_L+2L_XC_{SE}+2m'C_SL_X\right)+1\right)=0\end{aligned} \tag{22}$$

$$S_{SE}=\frac{1}{C_{SE}} \tag{23}$$

$$\begin{aligned}&2s^2L_X\left(s^2\left(2m'C_SL_X\right)+1\right)+\left(s^2\left(2mC_SL_X\right)+1\right)\left(2s^2L_X\right)=0\\&\Rightarrow C_SL_Xs^2\left(m+m'\right)+1=0\end{aligned} \tag{24}$$

$$\begin{aligned}&C_SL_Xs^2\left(m+m'\right)+1=0\rightarrow\\&s=\sqrt{\frac{-1}{C_SL_X}}\rightarrow\\&s=\pm\frac{j}{\sqrt{C_SL_X}}\end{aligned} \tag{25}$$

$$\begin{aligned}&s^6\left(4mm'C_S^2L_X^2L_L\right)+C_SL_Xs^4\left(4L_X+2L_L+4mm'C_SL_XS_{SE}\right)+\\&s^2\left(4L_X+2C_SL_XS_{SE}+L_L\right)+S_{SE}=0\end{aligned} \tag{26}$$

The equivalent impedance in the Laplace domain of the circuit in Fig. 22, from the open point on the left to the ground, can be written as in (20).

After simplifying the equivalent impedance further, the resulting fraction is shown in (21). The resonance condition can be obtained by equating the denominator to zero, as shown by (22).

This equation can be simplified further by dividing by C_{SE} and defining a new variable, as in (23).

For validation, if L_L and S_{SE} are set to equal zero, which simulates the ringing scenario in the absence of series capacitor and with line impedance ignored. The result is then shown in (24).

Recall that $m + m' = 1$, which results in (25).

This matches the ringing frequency as derived in [1].

Now that (22) has been validated, the equation can be rewritten to collect various terms of the polynomial. The result is shown in (26).

Note that an equation such as (26) with only even powers has either purely real roots or purely imaginary roots. Because all the coefficients are positive, the roots have to be purely imaginary. A total of six purely imaginary roots (three pairs of complex conjugates) will exist for (26). Fig. 23 provides the variation in the three roots (the other three have the same magnitude, but the opposite sign of the imaginary part) for a 220 kV fully transposed line and 75 percent shunt reactor compensation (with a neutral reactor sized to properly compensate for mutual capacitance) as the series compensation is varied from 0 percent to 90 percent compensation level.

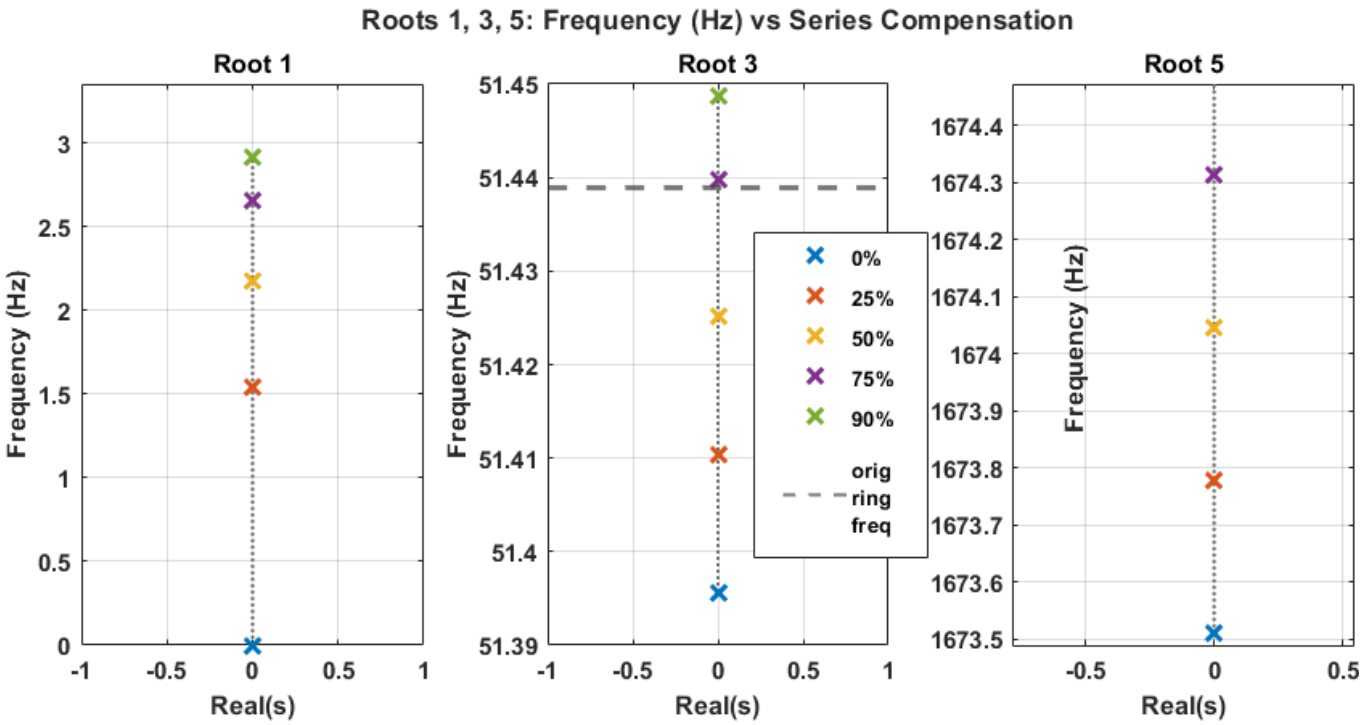

Fig. 23. Roots of (26).

From Root 3 (center plot in Fig. 23) variation, it is clear that the ringing frequency is not affected by series compensation. From the SAE simulation result shown in Fig. 24, where 50 percent series compensation was considered, it can be verified that the oscillation after SAE is dominated with the ringing frequency as determined by Root 3. Fig. 24 shows the raw voltage as well as the voltage filtered to remove the fundamental frequency.

Freq = 1/(1.3366 – 1.3168) = 50.5 Hz

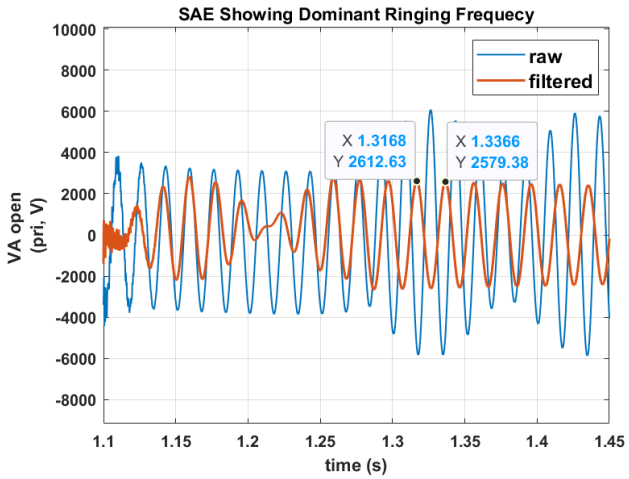

Fig. 24. Simulation for 75% shunt reactor compensated and 50% series-capacitor-compensated line showing dominant ringing frequency corresponding to Root 3.

VII. Acknowledgment

The authors gratefully acknowledge Dr. Normann Fischer, Dr. Armando Guzmán, Bernard Matta, Kamal Garg, Mark Feltis, Shashidhar Reddy Sathu, and Sathish Kumar Mutha for their careful review and helpful comments. We also thank Comisión Federal de Electricidad (CFE) for sharing field events and transmission line data.

VIII. References

[1] T. E. V. Ramirez, C. A. V. Nuñez, S. K. Harmukh, D. Schmidt, E. Clawson, O. A. Oliveros, and J. L. Eternod, "Reliable Open-Phase Fault Detection to Prevent Single-Pole Reclosing Onto Existing Faults," proceedings of the 48th Annual Western Protective Relay Conference, Spokane, WA, October 2024.

[2] M. R. Dadash Zadeh, I. Voloh, M. Kanabar, and Y. Xue, "An Adaptive HV Transmission Lines Reclosing based on Voltage Pattern in the Complex Plane," proceedings of the 65th Annual Conference for Protective Relay Engineers, College Station, TX, April 2012.

[3] A. M. Al-Rawi, "Simulation of secondary arcs in ehv systems employing single-pole autoreclosure," Student Thesis: Doctoral Thesis > PhD, Department of Electronic & Electrical Engineering, Univeristy of Bath, Bath, U.K., 1981.

[4] B. Kasztenny, D. Sharples, V. Asaro, and M. Pozzuoli, "Distance Relays and Capacitive Voltage Transformers – Balancing Speed and Transient Overreach," proceedings of the 54th Annual Georgia Tech Protective Relaying Conference, Atlanta, GA, May 2000.

[5] R. L. A. Reis, W. L. A. Neves, F. V. Lopes, and D. Fernandes Jr., "Coupling Capacitor Voltage Transformers Models and Impacts on Electric Power Systems: A Review," *IEEE Transactions on Power Delivery*, Vol. 34, Issue 5, October 2019, pp. 1874–1884. doi: 10.1109/TPWRD.2019.2908390.

[6] P. Datka, K. Narendra, H. Eriksson, A. Harjula, R. Le Roux, S. Srivastava, and P. Marken, "Transient Recovery Voltage (TRV) and Rate of Rise of Recovery Voltage (RRRV) of Line Circuit Breakers in Over Compensated Transmission Lines," proceedings of the CIGRE US National Committee 2017 Grid of the Future (GOTF) Symposium, October 2017.

[7] S. Chandankar and A. A. Bhole, "Sensitivity Analysis of TRV in Series Compensated Transmission Lines," proceedings of the 2017 2nd IEEE International Conference on Recent Trends in Electronics, Information & Communication Technology (RTEICT), Bangalore, India, May 2017.

[8] J. Giesbrecht, D. S. Ouellette, and C. F. Henville, "Secondary Arc Extinction and Detection Real and Simulated," proceedings of the 2008 IET 9th International Conference on Developments in Power System Protection (DPSP 2008), Glasgow, Scotland, May 2008.

IX. Biographies

Emma Clawson received her BS in electrical engineering, summa cum laude, from Washington State University in 2021. In 2020 she was hired as an intern at Schweitzer Engineering Laboratories, Inc. (SEL), where she transitioned to working as a power engineer in 2021. She has also worked briefly for Avista Utilities as part of an engineering development exchange program between Avista Utilities and SEL.

David Schmidt received his BS in physics from Vanderbilt University in 2000 and his ME in electrical engineering from the University of Idaho in 2017. He joined Schweitzer Engineering Laboratories, Inc. (SEL) in 2009 as a protection engineer and project manager in the SEL Engineering Services, Inc. (SEL ES) group, working on protection and control design and relay settings. He is presently a development engineer in research and development working on product development. He is a registered professional engineer in the states of Washington and California and a member of IEEE.

Sajal Kumar Harmukh received his B.Tech degree in electrical power engineering in 2012 from the Indian Institute of Technology Delhi in India, and his MS degree in electrical engineering in 2016 from the University of Illinois at Urbana-Champaign. Previously, he worked for NTPC Limited, India, as an assistant manager in the Operations and Maintenance department. He currently works as a power engineer at Schweitzer Engineering Laboratories, Inc.

Jordan A. Bell received his BSEE from Washington State University in 2006. He joined Schweitzer Engineering Laboratories, Inc. (SEL) in 2008 as a protection engineer in the SEL Engineering Services, Inc. (SEL ES) group. He is currently a senior engineer working on protection and control focusing on event report analysis, relay settings and coordination, fault studies, and model power system testing with a real-time digital simulator. He is a registered professional engineer in the state of Washington, a member of IEEE, and is active in the Power System Relaying and Control Committee (PSRC).

Omar A. Oliveros received his BS in electrical engineering from Universidad Autónoma de Puebla, Mexico. From 2005 to 2016, he worked as a protection engineer at Comisión Federal de Electricidad (CFE) where he performed electrical studies, protection schemes commissioning and testing, engineering design, and fault analysis in the transmission and generation divisions. He joined Schweitzer Engineering Laboratories, Inc. (SEL) in 2016 as technical support protection application engineer for the Mexico central region, then for the Central America and Caribbean regions, and is currently working as a Technology Director of SEL Latin America region.

Jean León Eternod is a field application engineer for Schweitzer Engineering Laboratories, Inc. (SEL) in Mexico City. Prior to joining SEL in 1998, he worked for the Comisión Federal de Electricidad (CFE) power systems studies office in protection and control corporate management. While with CFE from 1991 to 1998, he worked with wide-area network protection schemes, single-pole trip and reclose studies, and database validation for short circuit, load flow, and dynamic simulation. He received his BSEE from the National Autonomous University of Mexico (UNAM), where he also completed postgraduate course work in power systems. He received training in power system simulation from Power Technologies Inc. He has delivered technical papers for the summer meeting of the Mexican chapter of IEEE, Monterrey's Ibero-American Symposium on Protection of Electrical Power Systems (SIPSEP), AMIME Rotating Machinery Conference, Western Protective Relay Conference, and Texas A&M Protective Relay Conference in the fields of power system protection, simulation, and synchronized phasor measurement applications.

Jacob Smith is an electrical engineering intern at Schweitzer Engineering Laboratories, Inc. He is currently a student at Washington State University and is due to receive a BS in electrical engineering in 2026.

Colton Hubbell is currently a student at the University of Idaho and is expected to graduate in 2026 and due receive a BS in electrical engineering with an emphasis on power. He was hired by Schweitzer Engineering Laboratories, Inc. in 2025 as an electrical engineering intern in the Research and Development division.